frontiers | Frontiers in Marine Science

TYPE Original Research
PUBLISHED 16 February 2023
DOI 10.3389/fmars.2023.1101469

OPEN ACCESS

EDITED BY
Inna Sokolova,
University of Rostock, Germany

REVIEWED BY
Bo Gustafsson,
Stockholm University, Sweden
Songlin Liu,
South China Sea Institute of Oceanology (CAS), China

*CORRESPONDENCE
Jan Vanaverbeke
jvanaverbeke@naturalsciences.be

SPECIALTY SECTION
This article was submitted to Marine Biology, a section of the journal Frontiers in Marine Science

RECEIVED 17 November 2022
ACCEPTED 30 January 2023
PUBLISHED 16 February 2023

CITATION
Voet H, Soetaert K, Moens T, Bodé S, Boeckx P, Van Colen C and Vanaverbeke J (2023) N_2O production by mussels: Quantifying rates and pathways in current and future climate settings.
Front. Mar. Sci. 10:1101469.
doi: 10.3389/fmars.2023.1101469

N_2O production by mussels: Quantifying rates and pathways in current and future climate settings

Helena Voet[1,2], Karline Soetaert[3], Tom Moens[2], Samuel Bodé[4], Pascal Boeckx[4], Carl Van Colen[2] and Jan Vanaverbeke[1,2]*

[1]Royal Belgian Institute of Natural Sciences (RBINS), Operational Directorate Natural Environment, Marine Ecology and Management, Brussels, Belgium, [2]Marine Biology Research Group, Department of Biology, Ghent University, Ghent, Belgium, [3]Department of Estuarine and Delta Systems, Royal Netherlands Institute for Sea Research (NIOZ), Yerseke, Netherlands, [4]Isotope Bioscience Laboratory (ISOFYS), Department of Green Chemistry and Technology, Ghent University, Ghent, Belgium

Blue mussels (*Mytilus edulis*) are an abundant and economically important species across the North Sea. Partly because of their potent filter feeding and associated shell biofilm, they are able to influence and alter the surrounding marine ecosystem. As a result of proliferating offshore wind farms (OWFs), whose turbine foundations are rapidly colonised by suspension feeding artificial hard substrate communities dominated by *M. edulis*, as well as planned co-location strategies of these OWFs with mussel mariculture, their numbers will only increase towards the future. On top of these local stressors, global climate change is exerting additional pressure on the marine environment. This study focusses on the link between *M. edulis*, its microbial shell biofilm and the local nitrogen cycling by quantifying the magnitude and underlying pathways of mussel-associated nitrous oxide (N_2O) production. A set of closed-core incubations established nitrifier denitrification as the main chemical pathway of *M. edulis* related N_2O production, although ammonium, nitrite and nitrate all acted as possible precursors. Additional future-climate experiments revealed that blue mussel's total N_2O production, as well as its metabolic activity and the relative contribution of its shell biofilm, were affected by warming (+ 3°C), acidification (- 0.3 pH units), or the combination of both. Because the effects of temperature and acidity were often of an antagonistic nature, the results suggest a relatively small net effect on local N_2O production in future-climate marine environments. However, N_2O production rates were several orders of magnitude lower than other measured N species (NH_4^+, NO_2^- and NO_3^-), making substantial mussel-associated N_2 production likely. This would greatly affect the local eutrophication levels or even bioavailable nitrogen concentrations.

KEYWORDS

nitrous oxide - N2O, *Mytilus edulis*, climate change, biofilm, production pathways

1 Introduction

After carbon dioxide (CO_2) and methane (CH_4), nitrous oxide (N_2O) is an impactful long-lived greenhouse gasses (GHGs), substantially contributing to global warming (estimated 6 %) and to the depletion of the stratospheric ozone layer (IPCC, 2021). It has a long atmospheric lifetime (average of 114 years) and its warming effect on the global climate through radiative forcing (Global Warming Potential of 273 for a 100-year timescale) therefore persists for over a century after its emission (Smith and Sharp, 2012; Myhre et al., 2013; IPCC, 2021). N_2O is produced by (de) nitrifying bacteria and archaea in both terrestrial and aquatic environments, mainly associated with agricultural practices and invertebrate presence or activities (Mosier et al., 1998; Stein and Yung, 2003; Heisterkamp et al., 2010). The biogenic emission of N_2O by freshwater invertebrates is correlated with their feeding type, due to the denitrifying activity of ingested bacteria in the anoxic digestive system (Stief et al., 2009). In the marine environment, N_2O is emitted by denitrifying gut bacteria as well, but also by microbial biofilms on the surfaces of e.g. bivalves and gastropods (Heisterkamp et al., 2010; Heisterkamp et al., 2013). These shell biofilms can generate N_2O through three main pathways (Figure 1): (1) as a by-product of ammonium oxidation, the first step in (oxic) nitrification by ammonium-oxidising bacteria (AOB) and archaea (AOA), (2) as an intermediate in the reduction of nitrite during AOB- and AOA-mediated suboxic nitrifier denitrification and (3) as an intermediate in the reduction of nitrate during anoxic denitrification by heterotrophic bacteria. The latter comprises the final steps in the pathway of coupled nitrification-denitrification (CND), in which (heterotrophic) denitrification is carried out by a different set of actors compared to (autotrophic) nitrifier denitrification and nitrification (Figure 1).

An important shell-bearing organism in coastal ecosystems is the blue mussel *Mytilus edulis*. It has an important ecological relevance through its high filtration capacity and 'bio-engineering' role in habitat creation and food provision (Cranford, 2019; Degraer et al., 2020). In the North Sea, it is one of the main colonising species on artificial hard substrate [AHS] (De Mesel et al., 2015), readily available due to the proliferating European offshore wind farm [OWF] industry (IEA, 2019; GWEC, 2021). Partly due to the blue mussel's presence, these AHSs act as an artificial reef and as a biofilter, redirecting organic material from the water column towards the benthic environment (Slavik et al., 2019; Ivanov et al., 2021). Furthermore, this species has a high economical value because of its prominent role in aquaculture (Costello et al., 2020), a practice that might progressively be combined with OWF operations (Schupp et al., 2019; MSP, 2020) as a favourable way of minimising the impacted seafloor footprint (Buck and Langan, 2017; Steins et al., 2021).

All three of the N_2O-producing pathways (Figure 1) could potentially occur in and on the blue mussel. Firstly, *M. edulis* accommodates a selection of ingested denitrifying bacteria in its anoxic digestive system, where organic carbon and different N-species are readily available (Stief et al., 2009). Additionally, it has a microbial biofilm on the outer surface of its shell, within which a variable oxygenation allows different pathways of N_2O emission (Heisterkamp et al., 2010; Heisterkamp et al., 2013). Furthermore,

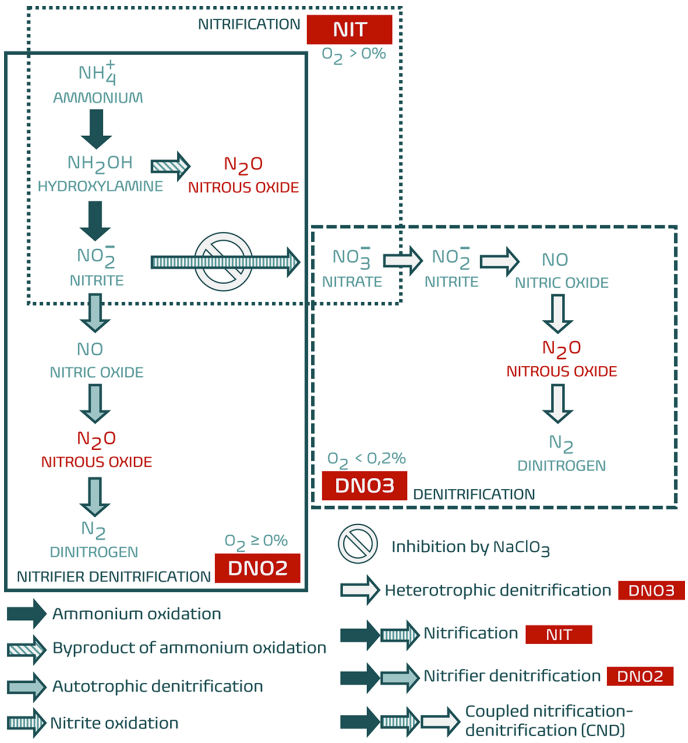

FIGURE 1
Relevant pathways in the marine nitrogen cycle with possible sources of N_2O emission and oxygenation demands. The result of a targeted inhibition by $NaClO_3$ is indicated. *NIT*: oxic nitrification (autotrophic); *DNO2*: suboxic nitrifier denitrification (autotrophic); *DNO3*: anoxic denitrification (heterotrophic) coupled to nitrification. *Adapted from* Zhu et al. (2013).

these biofilm emissions can be sustained through the pumping activity of the mussel replenishing its surroundings with nutrient-enriched waters (Heisterkamp et al., 2013). This could potentially decouple the shell biofilm's N_2O production from (outside) environmental nitrogen cycling and fluctuations, establishing a relatively stable capacity for N_2O emission. In an OWF or aquaculture environment, where mussels are typically present in high densities, this could potentially generate high local N_2O emissions (Voet et al., manuscript in preparation)[1].

The abundance of mussels could well rise towards the future due to their potential in offshore and integrated multi-trophic aquaculture projects (Avdelas et al., 2021). When investigating the production of a potent greenhouse gas by such a marine species, the link with marine climate change and its global effects on the oceanic environment needs to be taken into account. The IPCC predicts a sea surface temperature rise of ca. 3 °C and a drop in oceanic pH of ca. 0.3 by the end of this century (Bindoff et al., 2019; Fox-Kemper et al., 2021; IPCC, 2021), changing the biochemistry in marine environments and potentially affecting the N_2O emissions by mussel aggregations. The objective of this study was therefore to investigate the production of N_2O by *M. edulis* and its associated shell biofilm in current conditions and to describe the potential effects of seawater temperature and pH on both. This was done by experimentally (1) quantifying the relative contribution of the microbial shell biofilm to *M. edulis*' entire N_2O production and (2) unravelling the different chemical pathways and precursors of *M. edulis*' N_2O production. Experiments were performed in a fully-crossed design of temperature and pH, representing current and future climate conditions.

2 Methodology

2.1 Organism collection and incubation set-up

In summer 2018 and 2020, a respective total of 800 and 240 adult blue mussels (*Mytilus edulis*) with a mean soft tissue dry weight (± SD) of 0.79 ± 0.28 g were sampled from a *M. edulis* longline in an offshore aquaculture pilot project approximately 10 km off the Belgian coast (51°11.02'N - 02°39.88'E). All samples were stored in aerated seawater and transported to the experimental facilities within 4 hours.

On both occasions, organisms were evenly and randomly distributed across four identical aquaria (100 × 5 × 0 cm). These were equipped with a continuous flow-through mechanism, allowing the homogenisation of approximately 400 L natural seawater in circulation per system. All aquaria were continuously aerated and pre-set at laboratory conditions mimicking the *in situ* seawater salinity, temperature and pH at the time of sampling (34 PSU, 20°C and pH 7.96; LifeWatch Belgium, 2015). After an initial acclimatisation period of minimum 48 h under ambient conditions, both seawater temperature and pH were manipulated individually across the aquaria. This resulted in a 2 × 2 factorial design with four experimental treatments: a control treatment [CTRL: *in situ* temperature and pH], an ocean acidification treatment [OA: *in situ* temperature and lowered pH], an ocean warming treatment [OW: elevated temperature and *in situ* pH] and a climate change treatment [CC: combined elevated temperature and lowered pH].

For each treatment, stepwise manipulations were imposed over the course of three days, with a daily seawater temperature increase of 1°C and/or pH decrease of 0.1 pH unit. Seawater temperature was regulated using TECO TK2000 heaters and pH was manipulated through the controlled bubbling of 100 % CO_2 in the OA and CC treatment tanks using the IKS AquaStar aquaristic computer system, simultaneously logging temperature and pH records every 15 minutes throughout the six-week experiments (Table 1; Appendix A-Appendix B). This resulted in environmental conditions of +3°C and/or -0.3 pH units in the corresponding treatments compared to the control settings, reflecting the IPCC RCP-SSP8.5 projections for ocean warming and acidification towards the end of this century (Hoegh-Guldberg et al., 2014; IPCC, 2021). These conditions were maintained for six weeks and organisms were fed three times a week by adding 5 mL Shellfish Diet 1800® (Instant Algae® mix by Reed Mariculture Inc.) to each aquarium. Glass pH electrodes were calibrated weekly using Hanna Instruments™ NIST Reference Buffer Solutions (4.01 and 7.01) and each aquarium was sampled weekly to determine Total Alkalinity (TA) using a CONTROS HydroFIA™TA alkalinity system. One third of each flow-through system's water was renewed weekly. The carbonate chemistry of the seawater was calculated using CO_2SYS software (Pierrot et al., 2006) with the thermodynamic constants of Mehrbach et al. (1973).

2.2 Experimental procedures

2.2.1 Relative contribution of shell biofilm to N_2O production

Weekly, triplicated individual closed-core incubations were set up in each experimental treatment (CTRL, OA, OW and CC) to measure N_2O production by the mussel itself and its shell biofilm (see Appendix C: Experiment 1). Whole mussels [*WHOLE*] and dissected mussel shells [*SHELL*] were incubated separately, along with a control incubation without mussels or shells [*EMPTY*] to correct for background N_2O presence. An additional control consisted of whole mussels in a 1 % $ZnCl_2$ seawater solution inhibiting all biological activity [*ZNCL*] (Heisterkamp et al., 2013). Each incubation core of 1.5 L held one individual or dissected shell of one individual (except *EMPTY*), along with manipulated seawater from the respective treatment, and was kept at the correct temperature throughout 3h the incubations. A magnetic stirrer ensured an evenly mixed water column in the cores. Discrete 30 mL water samples were taken at the start and end of the closed-core incubations and stored at room temperature in dark conditions. Each sample filled, to overflowing, a 30 mL airtight serum bottle and was fixed with 100 µL saturated $HgCl_2$ solution for N_2O analysis. Quantification of dissolved N_2O was done by gas chromatography (SRI Instruments, ECD) and the N_2O production rates (PR) of whole organisms and dissected shells were calculated according to Equation 1:

1 Voet, H. E. E., De Luca, L. V., Vanaverbeke, J., and Soetaert, K. (manuscript in preparation). Modelling the combined effects of climate change on an offshore wind farm ecosystem with blue mussel (Mytilus edulis) aquaculture in multifunctional co-use.

$$PR\ (nmol\ ind^{-1}\ \ h^{-1}) = \frac{V\ (C_1 - C_0)}{(t_1 - t_0)} \qquad \text{Equation 1}$$

with V the volume (L) of the incubation core corrected for the biovolume of the whole organism or shell and with C_0 and C_1 the concentrations of N_2O (nmol L^{-1}) at the start and finish of the closed-core incubation, t_0 and t_1 (h), respectively. The relative contribution of the shell biofilm to whole animal N_2O production was calculated by dividing each *SHELL* PR by the corresponding *WHOLE* PR in each week and treatment.

2.2.2 Pathways of N_2O production: Nutrient flux and inhibition by $NaClO_3$

After three and six weeks of manipulations [*WK3* and *WK6*, respectively], triplicated closed-core incubations with individual whole organisms were set up and sampled as described above (see Appendix C: Experiment 2). Along with biomass-specific N_2O production rates [PRB] (calculated according to Equation 2), NH_4^+, NO_2^- and NO_3^- concentrations were measured through discrete sampling (25 mL; automated colorimetric analyses performed on SKALAR SAN++ CFA) at the start and finish of closed-core incubations, with and without the addition of 20 mM $NaClO_3$ to inhibit CND (Belser and Mays, 1980; see Figure 1). $NaClO_3$ inhibits the oxidation of nitrite (NO_2^-) to nitrate (NO_3^-) in the nitrification pathway (Figure 1), meaning N_2O is produced either though nitrification (as a by-product during ammonium oxidation) or through nitrifier denitrification (as result of denitrification of nitrite; Tallec et al., 2008), as well as through denitrification of nitrate already present in the incubation core (Figure 1).

Nutrient flux was calculated according to Equation 3;

$$PRB\ (nmol\ g^{-1}DW\ h^{-1}) = \frac{V\ (C_1 - C_0)}{DW\ (t_1 - t_0)} \qquad \text{Equation 2}$$

$$\text{Nutrient flux}\ (\mu mol\ g^{-1}DW\ h^{-1}) = \frac{V\ (C_1 - C_0)}{DW\ (t_1 - t_0)} \qquad \text{Equation 3}$$

with parameters identical as in Equation 1, C the concentration of N_2O (nmol L^{-1}) and nutrients NH_4^+, NO_2^- or NO_3^- (µmol L^{-1}) in Equation 2 and Equation 3, respectively, and DW the dry weight (g) of the mussel's soft tissue.

2.2.3 Pathways of N_2O production: ^{15}N stable isotope tracer experiments

Three different labelled N-tracer treatments were designed to distinguish the production of double-^{15}N-labelled N_2O ($^{46}N_2O$) from either nitrification [*NIT*], nitrifier denitrification [*DNO2*] or CND [*DNO3*], in which NH_4^+, NO_2^- or NO_3^- act as a precursor to N_2O production, respectively (Table 2 and Figure 1). The composition of these N-tracer treatments, in which ^{15}N was introduced using either $^{15}NH_4Cl$ [*NIT*], $Na^{15}NO_2$ [*DNO2*] or $Na^{15}NO_3$ [*DNO3*], and the resulting concentrations in the incubation cores were identical to those in Heisterkamp et al (2013; adapted in Table 2).

TABLE 1 Average (± SD) seawater temperature (°C), pH and salinity of four experimental treatments.

	CTRL	OW	OA	CC
Temperature (°C)				
Summer 2018	20.02 ± 0.13	23.15 ± 0.24	19.99 ± 0.29	23.13 ± 0.31
Summer 2020	19.92 ± 0.27	23.07 ± 0.36	20.01 ± 0.34	23.11 ± 0.49
pH				
Summer 2018	7.96 ± 0.01	7.97 ± 0.02	7.65 ± 0.02	7.65 ± 0.01
Summer 2020	7.96 ± 0.02	7.96 ± 0.02	7.63 ± 0.05	7.65 ± 0.01
Salinity				
Summer 2018	32.9 ± 0.5	33.8 ± 0.5	32.4 ± 0.4	33.0 ± 0.5
Summer 2020	33.9 ± 1.4	34.6 ± 0.7	33.7 ± 1.1	34.5 ± 0.7

[CTRL, control; OW, ocean warming; OA, ocean acidification and CC, climate change] throughout both experiments.

TABLE 2 Nitrogen tracer treatments *NIT*, *DNO2* and *DNO3* with the targeted N_2O-producing pathway and precursor, the concentrations of ^{15}N and ^{14}N added to the tracer treatments and the possible combinations of ^{14}N and ^{15}N to form $^{45}N_2O$ and $^{46}N_2O$, respectively.

	NIT	DNO2	DNO3
Pathway	Nitrification	Nitrifier denitrification	Coupled nitrification- denitrification
Precursor	oxidation of NH_4^+	denitrification of NO_2^-	denitrification of NO_3^-
^{15}N added	$^{15}NH_4^+$ (50µM)	$^{15}NO_2^-$ (50µM)	$^{15}NO_3^-$ 50µM)
^{15}N added	$^{14}NO_2^-$ (500µM)	$^{14}NO_3^-$ (500µM)	–
$^{45}N_2O$	$^{14}NH_4^+/^{14}NH_X^- + ^{15}NH_4^+$	$^{14}NO_X^- + ^{15}NO_2^-$	$^{14}NO_X^- + ^{15}NO_3^-$
$^{45}N_2O$	$^{15}NH_X^+ + ^{15}NH_4^+$	$^{15}NO_2^- + ^{15}NO_2^-$	$^{15}NO_3^- + ^{15}NO_3^-$

$^{14}NO_X^-$ represents either $^{14}NO_2^-$ or $^{14}NO_3^-$. *Adapted from* Heisterkamp et al. (2013).

Before manipulations took place [*WK0*] and at *WK3* and *WK6*, triplicated closed-core incubations for all three N-tracers were set up in all four experimental treatments (CTRL, OA, OW and CC; see Appendix C: Experiment 3). The 125mL incubation cores held one individual in seawater from its respective experimental treatment amended with the respective N-tracer. Cores were incubated for 4 hours on a shaking table to ensure adequate mixing. Hourly, 1mL samples were taken with a surgical syringe and transferred to 12mL He-flushed exetainers. These were prefilled with 100µL saturated $HgCl_2$ and 20 nmol natural N_2O with known isotopic composition. The $HgCl_2$ was added to fixate the N_2O, while the addition of unlabelled N_2O ensured the detection limit of the isotope ratio mass spectrometer was reached. Since only 4 % of the core volume was sampled by the end of the incubation, under-pressure was not considered to be an issue, and the withdrawn volume was not replaced. The excess $^{45}N_2O$ and $^{46}N_2O$ content was determined from the $^{45}N_2O/^{44}N_2O$ and $^{46}N_2O/^{44}N_2O$ ratio of the samples compared to a reference N_2O spiked blank sample using a ANCA-TGII interfaced with a SerCon 20-20 IRMS (SysCon electronics) with cryogenic trapping and focusing of samples. Production of $^{44}N_2O$ could not be determined in this assay due to the presence of the added 20 nmol N_2O spike. The linear increase of $^{45}N_2O$ and $^{46}N_2O$ over time was used to calculate net PRB (nmol g^{-1}DW h^{-1}). The contribution of the different pathways to the total ^{15}N-labelled N_2O production was calculated by dividing the respective $^{46}N_2O$ PRB by the sum of $^{45}N_2O$ and $^{46}N_2O$ PRB in each N-tracer experiment.

2.2.4 Shell biofilm oxygen microprofile

As a proxy for metabolic activity of shell biofilms, a vertical oxygen profile of the microbial biofilm on three replicate *M. edulis* shells was measured before seawater manipulations started [*WK0*] and in each experimental treatment after three and six weeks of manipulations [*WK3* and *WK6*, respectively]. Individuals were carefully dissected with a scalpel to isolate the mussel shell without damaging the associated biofilm and dissected shells were placed in aerated seawater from the respective experimental treatments. A Unisense™ MicroProfiling System was used to position the sensor tip of a PyroScience™ retractable fiber oxygen microsensor on the shell surface and a vertical dissolved oxygen concentration profile was recorded in increments of 50 or 100 µm through the biofilm between 0-3000 µm above the shell surface. Oxygen microprofiles were measured at three random positions on the shell of each replicate organism and conducted in dark conditions to avoid net oxygen production.

2.3 Data analysis

The effect of temperature (current or elevated) and pH (current or lowered) on the production of N_2O in the *WHOLE*, *SHELL*, $NaClO_3$-inhibited and non-inhibited incubations was investigated using linear mixed effects models, with incubation core and/or experimental week added as a random factor in the models. If none of the random factors could explain left-over variance, a linear regression model was fitted. The effect of temperature, pH and experimental week (*WK3* or *WK6*) on nutrient flux was analysed using linear regression models. Significance of the two-way interaction 'temperature x pH' and *post-hoc* pairwise comparison of the group means was used to identify possible combination effects of increased temperature and lowered pH. Normality of the residuals and model assumptions were checked using Shapiro-Wilk, Gaussian error distributions were used and model selection was based on the parametric bootstrap and Kenward Roger methods for mixed model comparison (Halekoh and Højsgaard, 2014) or on the backwards selection procedure for linear regression models. Statistical analyses were conducted using R v3.6.1 (R Core Team, 2019), linear mixed effects models were built using the R package *lme4* (Bates et al., 2015) and linear regression models were fitted using the *stats* package (R Core Team, 2019).

To test for differences between oxygen microprofiles between experimental treatments in *WK3* and *WK6* (to keep a balanced design), a multivariate matrix was constructed with the oxygen concentrations at each distance above the shell (Widdicombe et al., 2013). Differences in the shell biofilm oxygen microprofiles were tested using permutational ANOVA (PERMANOVA) with experimental treatment and week as fully-crossed factors and with all profiles on all shells considered as replicates within the Euclidian distance matrix. For all significant PERMANOVA factors, *post-hoc* pairwise testing was used and homogeneity of multivariate dispersion was tested using PERMDISP. The SIMPER routine was used to identify which distances from the shell contributed most to any observed differences. Multivariate analyses were carried out in Primer v6.0 with PERMANOVA+ add-on software (Clarke and Gorley, 2006; Anderson et al., 2008).

3 Results

Mean seawater temperature (± SD) in CTRL treatments was 19.97 ± 0.20°C and ranged between 23.07 ± 0.36°C and 23.15 ± 0.24°C in the warmed treatments (OW and CC). Mean seawater pH (± SD) in acidified treatments (OA and CC) ranged between 7.63 ± 0.05 and 7.65 ± 0.02, compared to an average CTRL seawater pH of 7.96 ± 0.02 (Table 1; Appendix A - Appendix B). Seawater salinity differed slightly between the treatments but was well within the natural occurring salinity range. The total alkalinity (TA) fluctuated according to the pH levels (1985-2123 µmol kg^{-1}) and the average aragonite/calcite seawater saturation states (Ω; ± SD) ranged between 1.70 ± 0.25 – 2.97 ± 0.52 in the non-acidified treatments and between 0.82 ± 0.16 – 1.51 ± 0.24 in the acidified treatments (Table 3).

For an overview of ecophysiological effects of increased temperature and lowered seawater pH on *M. edulis*, see Voet et al. (2021). In this study, the same experimental treatments (CTRL, OW, OA and CC) were imposed for six weeks. Significant results included a decreased survival rate and growth in acidified treatments, enhanced growth rates in warmed treatments and an additive effect of higher temperatures and lower pH levels on respiration and clearance rates (Voet et al., 2021).

3.1 Relative contribution of shell biofilm to N_2O production

In all treatments, N_2O was produced in both the *WHOLE* and *SHELL* incubations, whereas no N_2O production was measured in the poisoned *ZNCL* incubations. In CTRL, whole animals produced on

TABLE 3 Average (± SD) seawater carbonate chemistry of four experimental treatments.

	CTRL	OW	OA	CC
TA (µmol kg^{-1})				
Summer 2018	2107 ± 248	2113 ± 268	1985 ± 280	2038 ± 317
Summer 2020	2119 ± 229	2123 ± 264	1996 ± 264	2048 ± 315
pCO_2 (µatm)				
Summer 2018	652 ± 65	650 ± 59	1361 ± 178	1420 ± 208
Summer 2020	656 ± 90	664 ± 53	1421 ± 216	1412 ± 246
C_T (µmol kg^{-1})				
Summer 2018	1967 ± 231	1951 ± 245	1951 ± 276	1991 ± 312
Summer 2020	1976 ± 224	1960 ± 243	1963 ± 260	1996 ± 312
Ω_A				
Summer 2018	1.70 ± 0.25	1.95 ± 0.34	0.82 ± 0.14	0.96 ± 0.17
Summer 2020	1.72 ± 0.19	1.94 ± 0.33	0.82 ± 0.16	0.99 ± 0.16
Ω_C				
Summer 2018	2.63 ± 0.39	2.97 ± 0.52	1.27 ± 0.22	1.46 ± 0.26
Summer 2020	2.65 ± 0.29	2.96 ± 0.50	1.27 ± 0.24	1.51 ± 0.24

[CTRL, control; OW, ocean warming; OA, ocean acidification and CC, climate change] throughout both experiments, Total Alkalinity (TA; µmol kg^{-1}); partial pressure of CO_2 (pCO_2; µatm); total inorganic carbon concentration (C_T; µmol kg^{-1}) and saturation state of the seawater with respect to aragonite (Ω_A) and calcite (Ω_C).

average (± SD) 4.55 ± 0.18 nmol N_2O ind^{-1} h^{-1} and throughout the experiment, the shell biofilm contribution ranged between 65-75% (Figure 2). In OW, the average *WHOLE* production rate gradually increased from 5.47 ± 0.23 to 15.84 ± 0.48 nmol N_2O ind^{-1} h^{-1} over six weeks, while the shell biofilm contribution remained stable at 68% (Figure 2). In both acidified treatments, the relative contribution of the shell biofilm to whole organism N_2O production decreased over time. In OA, the *WHOLE* N_2O production rate was stable throughout the experiment (mean 5.79 ± 0.33 nmol N_2O ind^{-1} h^{-1}), but the contribution of the shell biofilm decreased from 63% to 23% over the course of six weeks (Figure 2). Whole animals in CC produced on average 9.10 ± 1.82 nmol N_2O ind^{-1} h^{-1}, while the associated shell biofilm contribution decreased from 60% to 12% over time, after an initial rise to 65% in the second week of experiments. Overall, temperature and pH had a significant, antagonistic effect on the parts of the animal that emitted N_2O, with an increasing production in warmer environments and a decreasing production in acidified or combined climate change conditions (Table 4).

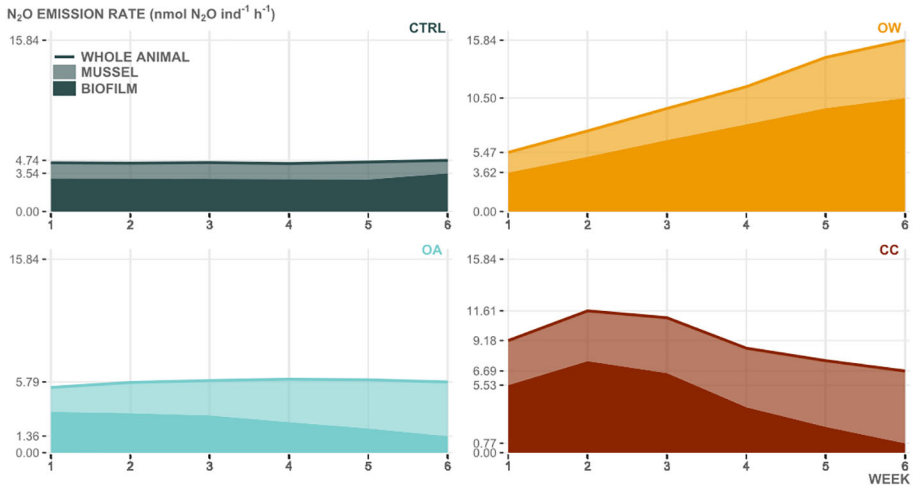

FIGURE 2
Estimated mean relative contribution of dissected *Mytilus edulis* shells [*SHELL*] to whole animal [*WHOLE*] N_2O emission rates (nmol N_2O ind^{-1} h^{-1}) in four experimental treatments [CTRL, control; OA, ocean acidification; OW, ocean warming and CC: climate change]. Relative contribution of *M. edulis* itself [*MUSSEL*] represents the calculated difference between the two.

TABLE 4 Structure of final linear mixed effects models for N_2O production [nmol N_2O ind^{-1} h^{-1}] by whole animals [*WHOLE*] and shell biofilms [*SHELL*]: significance of fixed effects Temperature (TEMP), pH (PH) and two-way interaction (TEMP x PH), and identity of random effects, including random intercept (format = 1|random) and potential random slope (format = 1+fixed|random).

FIXED EFFECT Temperature	FIXED EFFECT pH	FIXED EFFECT Temperature × pH	RANDOM EFFECT
WHOLE			
p=0.004	**p=0.033**	p=0.387	1+TEMP×PH|WEEK
SHELL			
p=0.004	p=0.379	**p=0.007**	1+TEMP×PH|WEEK

Significance indicated in bold. [WEEK = experimental week].

3.2 Pathways of N_2O production

3.2.1 Nutrient flux and inhibition of coupled nitrification-denitrification

When the CND pathway was inhibited by the addition of $NaClO_3$, average N_2O production rates were 4 to 16 times higher compared to incubations where the inhibitor was absent (Figure 3). Regardless of the presence of the inhibitor, temperature and pH had an antagonistic effect on the production of N_2O by *M. edulis* and the highest average N_2O production rates were measured in OW (Figure 3 and Table 5).

Inhibition by $NaClO_3$ significantly lowered ammonium flux, which additionally decreased significantly in *WK6* compared to *WK3* (Figure 3 and Table 6). Lowered pH and elevated temperature antagonistically affected ammonium flux (production or oxidation rates; Table 6), with the lowest average NH_4^+ flux in OW and a significantly higher flux when combined with lowered pH in CC (Figure 3).

There was no significant effect of the inhibitor $NaClO_3$ on nitrite flux and in general, nitrite flux decreased with time (Figure 3 and Table 6). Elevated temperature and lowered pH significantly increased NO_2^- flux (Table 6).

Nitrate flux was negative across all experimental treatments and not affected by the presence of the inhibitor (Figure 3 and Table 6). Nitrate consumption (negative flux) significantly increased with time and the significant decreasing effect of a lowered pH was further amplified when combined with an elevated temperature in CC (Table 6).

3.2.2 N_2O precursors: ^{15}N stable isotope tracers

$^{45}N_2O$ and $^{46}N_2O$ was detected in all ^{15}N-tracer experiments across all treatments and weeks, showing that NH_4^+, NO_2^- and NO_3^- all serve as potential precursors and nitrification, nitrifier denitrification and coupled nitrification-denitrification (respectively) all serve as potential pathways of N_2O production by *M. edulis* and its shell biofilm (Table 7 and Figure 4).

In the *NIT* incubations, targeting the production of N_2O through nitrification (precursor NH_4^+), no or very low amounts of $^{46}N_2O$ (0.00 – 0.09 nmol $g^{-1}DW$ h^{-1}) were produced across all experimental treatments and weeks (Table 7 and Figure 4). The contribution of nitrification to the total ^{15}N-labelled N_2O production ($^{46}N_2O$ + $^{45}N_2O$) by *M. edulis* and its shell biofilm in this series of experiments was very low, ranging between 1 % in CTRL to 3 % in OA. The production rate of $^{45}N_2O$, on the other hand, was ± 10 to 500 times higher (0.03 – 2.95 nmol $g^{-1}DW$ h^{-1}), started after an initial lag phase of 3 hours (Figure 4 and Table 7) and was the result of either random isotope paring, nitrifier denitrification or CND (Table 2).

The *DNO2* incubations, targeting nitrifier denitrification (precursor NO_2^-), showed the highest average $^{46}N_2O$ production rates of all ^{15}N-tracer treatments, with highest average values (2.08 ± 0.96 nmol $g^{-1}DW$ h^{-1}) recorded in CC after 6 weeks (Table 7). Nitrifier denitrification contributed, on average, 46 % to the total labelled N_2O production of whole animals in CTRL and up to 59 % the OA treatment. In general, the $^{45}N_2O$ production rates were ± 1.2 to 3 times lower compared to $^{46}N_2O$ and produced by the combination of $^{15}NO_2^-$ with $^{14}NO_3^-$ or $^{14}NO_2^-$ present or produced during the incubation (Table 7 and Figure 4).

Average $^{46}N_2O$ production rates in *DNO3* incubations, targeting the CND pathway (precursor NO_3^-), was relatively high at the start of the experiment (*WK0*; 0.12 ± 0.18 nmol $g^{-1}DW$ h^{-1}) and contributed approximately 40 % of the total labelled N_2O production in that week. In subsequent weeks, $^{46}N_2O$ production rates decreased 2- to 42-fold and all manipulated treatments had higher average $^{46}N_2O$ production rates compared to CTRL (Table 7 and Figure 4). On average, CND contributed between 4 % in CRTL up to 15 % in OW in the subsequent weeks. Average $^{45}N_2O$ production rates were 2 to 46 times higher across all experimental treatments compared to $^{46}N_2O$ and occurred in the *DNO3* tracer treatment as a result of the random pairing of $^{15}NO_3^-$ with $^{14}NO_3^-$ or $^{14}NO_2^-$ that were present or produced during the incubation (Tables 2, 7).

3.2.3 Oxygen microprofile

The biofilm oxygen microprofiles differed significantly between experimental treatments (PERMANOVA; pseudo-F=93.98; p=0.001), while the effect of week or the 2-way interaction of both was not significant (PERMANOVA; pseudo-F=0.92 and 1.23, respectively; both p>0.29). Pairwise testing revealed significant differences in oxygen microprofiles between all experimental treatments (p=0.001), except for the profiles measured in OA and CC (p=0.24). SIMPER revealed that at least 90% of the differences between CTRL and the other experimental treatments could be attributed to the first 600µm above the shell surface. In OW, oxygen concentrations above the shell declined faster and stronger, while in both acidified treatments (OA and CC), the onset of the decline in oxygenation was closer to the shell surface (biofilm thickness declined) and the magnitude of the decline was lower (net biofilm oxygen consumption decreased) (Figure 5).

10.3389/fmars.2023.1101469

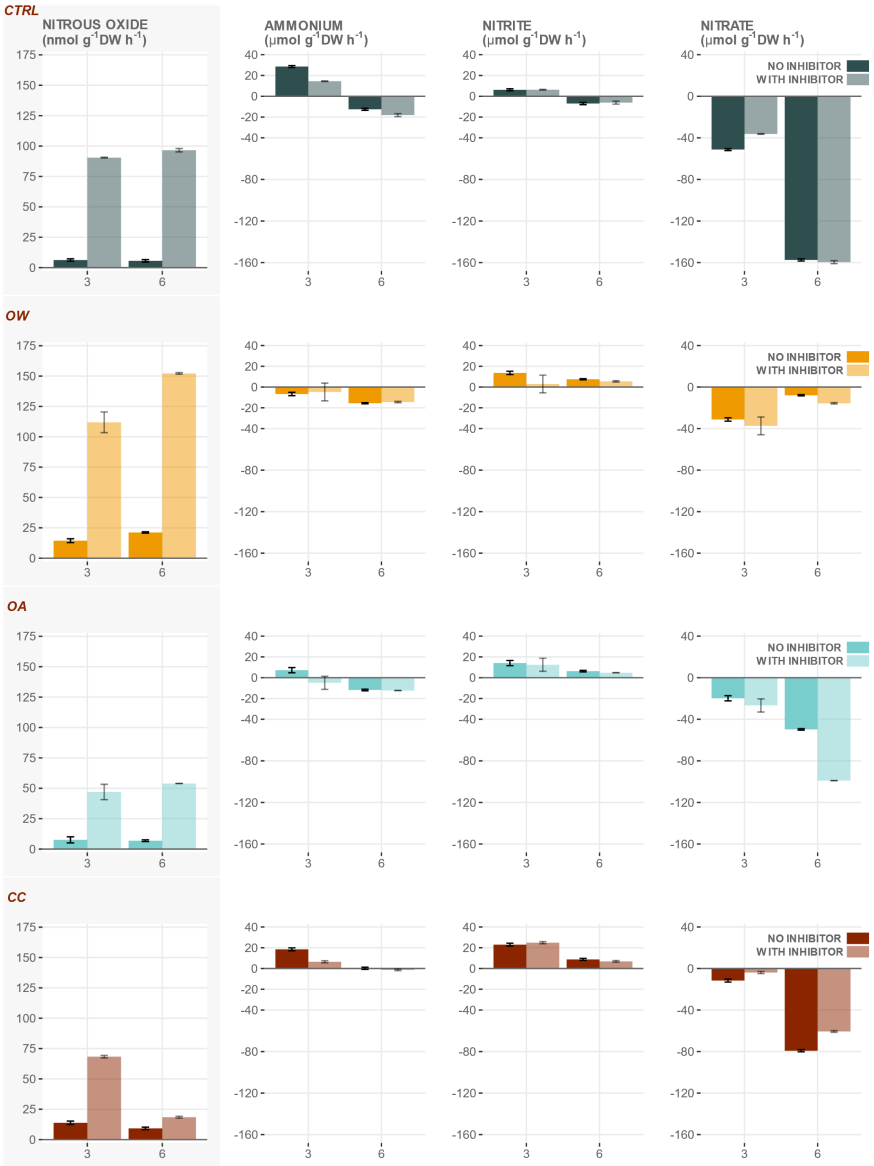

FIGURE 3
N_2O production rates (nmol g^{-1}DW h^{-1} ± SE) and nutrient flux (µmol g^{-1}DW h^{-1} ± SE) of whole animals incubated with and without the addition of $NaClO_3$, inhibiting the oxidation of nitrite to nitrate, in four experimental treatments [CTRL, control; OW, ocean warming; OA, ocean acidification and CC,: climate change]. *Note different scale and unit in left panels.*

4 Discussion

This study confirmed the contribution by the abundant and economically important blue mussel *Mytilus edulis* to marine N_2O production (Stief et al., 2009; Heisterkamp et al., 2010; Bonaglia et al., 2017), as well as the relative importance of shell biofilms in this process (Heisterkamp et al., 2013). Our results on the magnitude and underlying processes of this N_2O production show that nitrification, nitrifier denitrification and coupled nitrification-denitrification all served as potential pathways in N_2O production. In contrast to earlier research by Heisterkamp et al. (2013) on dissected shell biofilms, nitrification of NH_4^+ was not an important contributor to the total production by both

TABLE 5 R^2 of final linear regression models with significance of Temperature (TEMP), pH (PH), two-way interaction (TEMP x PH) and week (WEEK) in incubations with and without inhibitor $NaClO_3$ for production of N_2O [nmol g^{-1}DW h^{-1}].

	R^2	temp	pH	TEMPxPH	WEEK
N_2O [nmol g^{-1}DW h^{-1}]					
With $NaClO_3$	0.67	p=0.631	**p=0.007**	**p=0.037**	p=0.936
Without $NaClO_3$	0.76	**p=0.010**	p=0.405	**p=0.002**	p=0.858

Significance is indicated in bold.

TABLE 6 R^2 of final linear regression models with significance of Temperature (TEMP), pH (PH), two-way interaction (TEMP x PH), week (WEEK) and addition of inhibitor sodium chlorate ($NaClO_3$) for nutrient flux (ammonium NH_4^+, nitrite NO_2 and nitrate NO_3) [µmol g^{-1} DW h^{-1}].

	R^2	TEMP	PH	TEMPxPH	WEEK	$NaClO_3$
NH_4^+ µmol g^{-1}DW h^{-1}]						
	0.82	**p=0.002**	**p<0.001**	**p<0.001**	**p<0.001**	**p=0.003**
NO_2^- µmol g^{-1}DW h^{-1}]						
	0.65	**p<0.001**	**p<0.001**	p=0.734	**p<0.001**	p=0.244
NO_3^- µmol g^{-1}DW h^{-1}]						
	0.83	p=0.459	**p<0.001**	**p<0.001**	**p<0.001**	p=0.524

Significance is indicated in bold.

the mussels and its shell biofilm. Additionally, we suggest that future climate change will not substantially affect total N_2O production by blue mussels as the increase caused by higher temperatures is counteracted by a decreased shell biofilm activity due to ocean acidification and overall, N_2O production declined over time in the climate change environment.

4.1 Pathways and contributions to N_2O production

The current climate [CTRL] N_2O production of blue mussels (including their associated shell biofilm) was in line with other studies (e.g. Heisterkamp et al., 2010; Heisterkamp et al., 2013; Gárate et al., 2019) and exclusively biological, as $ZnCl_2$ poisoning fully inhibited N_2O production. The shell biofilm contribution to total N_2O production by *M. edulis* was important (± 70 %) and remained stable through time, as did the total N_2O production rate. Although still a considerable contribution, the partitioning measured in this study was lower than previously reported by Heisterkamp et al. (2013), where N_2O production originated almost exclusively from the shell biofilm (± 94 %). Possibly, methodological differences such as the use of natural seawater and a regular feeding regime in our experiments could have prompted the adept filter feeder *M. edulis*, with an established rich intestinal microbial system capable of considerable N_2O production, to continue to do so throughout the duration of this experiment.

Nitrifiers, a combination of ammonium-oxidising bacteria and archaea, produce N_2O during nitrification in oxic environments and during nitrifier denitrification in suboxic environments. Another set of

TABLE 7 $^{45}N_2O$ and $^{46}N_2O$ production rate (nmol g^{-1}DW h^{-1} ± SD) of whole animals before seawater manipulations started [*WK0*] and after three [*WK3*] and six [*WK6*] weeks of manipulations with three N-tracer targeting nitrification [*NIT*], nitrifier denitrification [*DNO2*] or coupled nitrification-denitrification [*DNO3*], in which NH_4^+, NO_2^- or NO_3^- act as a precursor to N_2O emission, respectively, in four experimental treatments.

		CTRL	OW	OA	CC
NIT					
WK0	$^{45}N_2O$ $^{46}N_2O$	0.536 ± 0.277 0.001 ± 0.007			
WK3	$^{45}N_2O$ $^{46}N_2O$	0.768 ± 0.789 0.014 ± 0.015	0.294 ± 0.150 0.000 ± 0.004	0.501 ± 0.510 0.003 ± 0.012	0.300 ± 0.057 0.004 ± 0.010
WK6	$^{45}N_2O$ $^{46}N_2O$	2.263 ± 2.074 0.019 ± 0.003	0.032 ± 0.049 0.004 ± 0.007	2.949 ± 1.562 0.086 ± 0.121	0.382 ± 0.173 0.006 ± 0.004
DNO2					
WK0	$^{45}N_2O$ $^{46}N_2O$	0.545 ± 0.472 1.479 ± 1.417			
WK3	$^{45}N_2O$ $^{46}N_2O$	0.910 ± 1.254 1.137 ± 1.291	0.365 ± 0.366 0.317 ± 0.332	0.343 ± 0.084 0.415 ± 0.069	0.473 ± 0.408 0.724 ± 0.799
WK6	$^{45}N_2O$ $^{46}N_2O$	2.309 ± 1.811 0.622 ± 0.436	0.793 ± 0.699 1.199 ± 0.966	0.359 ± 0.275 0.590 ± 0.491	1.540 ± 0.970 2.081 ± 0.956
DNO3					
WK0	$^{45}N_2O$ $^{46}N_2O$	0.182 ± 0.126 0.119 ± 0.110			
WK3	$^{45}N_2O$ $^{46}N_2O$	0.131 ± 0.032 0.003 ± 0.061	0.294 ± 0.200 0.040 ± 0.045	0.058 ± 0.065 0.007 ± 0.010	0.069 ± 0.078 0.021 ± 0.027
WK6	$^{45}N_2O$ $^{46}N_2O$	0.145 ± 0.126 0.008 ± 0.012	0.359 ± 0.355 0.072 ± 0.092	0.651 ± 0.189 0.026 ± 0.006	0.391 ± 0.431 0.019 ± 0.015

[CTRL, control; OA, ocean acidification; OW, ocean warming and CC, climate change].

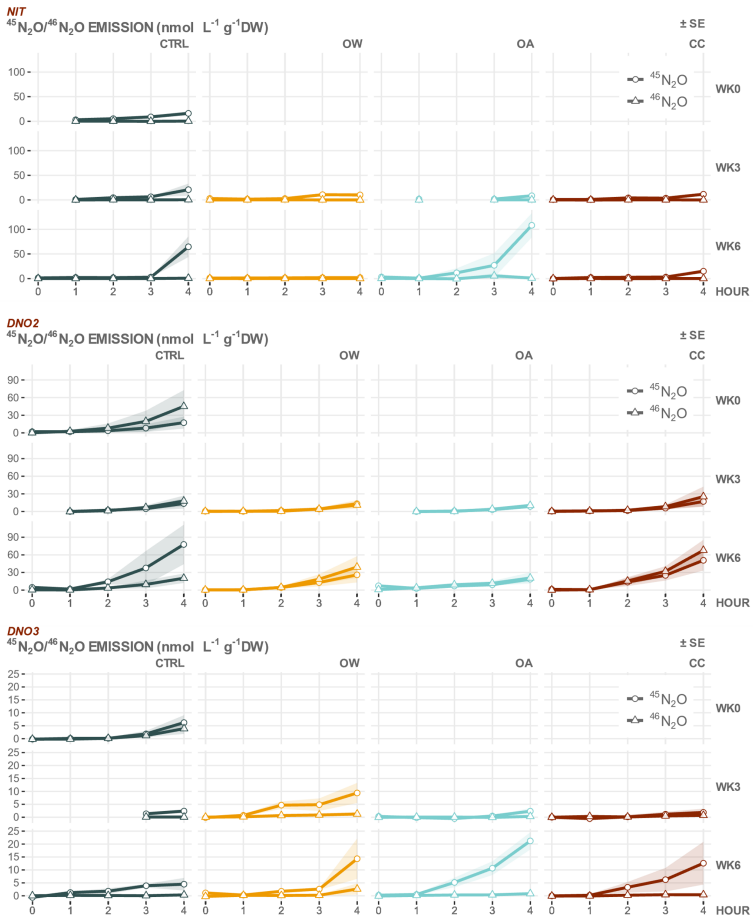

FIGURE 4
$^{45}N_2O$ (circles) and $^{46}N_2O$ (triangles) emission (nmol L^{-1} g^{-1}DW ± SE *shaded area*) of *M. edulis* before seawater manipulations [*WK0*] and after three [*WK3*] or six [*WK6*] weeks of manipulations with 3 N-tracers targeting nitrification [*NIT*], nitrifier denitrification [*DNO2*] or coupled nitrification-denitrification [*DNO3*], in which NH_4^+, NO_2^- or NO_3^- act as a precursor to N_2O emission, respectively, in 4 experimental treatments [CTRL: control, OA: ocean acidification, OW: ocean warming and CC: climate change]. Missing data due to faulty GC-IRMS. *Note difference in scale.*

bacteria, denitrifiers, produce N_2O during anaerobic denitrification in anoxic environments, comprising the final steps of CND. These three pathways are considered to be the main oceanic sources of N_2O production, while the main sink is the further reduction of N_2O to N_2 by (nitrifier) denitrification in sub- or anoxic environments (Bange et al., 2010). In this study, each of these three N_2O producing pathways were observed. Contrary to Heisterkamp et al. (2013), where only dissected shells were used in a similar experiment, nitrification apparently did not play as an important role when whole animals (incl. shell biofilm) were incubated. Most likely, the presence of the living and digesting animal itself caused the resulting total N_2O production to lean towards a more prominent inclusion of anoxic or suboxic pathways.

Denitrification of nitrite, targeted by the DNO2 precursor incubations, was the most dominant pathway of N_2O production by *M. edulis* in the current climate scenario, corroborating the findings of Heisterkamp et al. (2013). Production of N_2O in the presence of $NaClO_3$, actively preventing the oxidation of nitrite to nitrate, was on average an order of magnitude higher than without the inhibitor present. As such, we suggest that the availability of nitrite might be a limiting factor in the production of N_2O and that incomplete (nitrifier) denitrification of nitrite, where further reduction to N_2 has not (yet) happened, is indeed a major pathway of N_2O production by *M. edulis* and its biofilm. An overestimation of said denitrification due to anaerobic ammonium oxidation (anammox), where ammonium oxidises to N_2 using nitrite under anoxic conditions, was assumed negligible since no anammox activity has been associated with mussel biofilms before (Marzocchi et al., 2021).

Denitrification of nitrite can be associated with the presence of *M. edulis* in different ways, both in and on the organism. The incomplete denitrification of nitrite to N_2O by denitrifiers in the mussel's anoxic digestive system could be the result of a high lysozyme activity, cutting short the denitrification pathway (Birkbeck and McHenery, 1982; Heisterkamp et al., 2013; Gárate et al., 2019). Additionally, this last step in the nitrifier denitrification pathway has only be attributed to a certain genus of nitrifying bacteria, *Nitrosomonas* sp., whose biofilm presence and/or (differential) activity is related to oxygen and nutrient availability (Schramm et al., 2000; Shrestha et al., 2002) and substrate affinity and availability (Foesel et al., 2008; Zhu et al., 2013). With the variable oxygenation of the shell biofilm measured in this study in mind, this could further explain why the produced N_2O is not always readily reduced to N_2 in a heterogeneous microbial biofilm on *M. edulis*'s outer

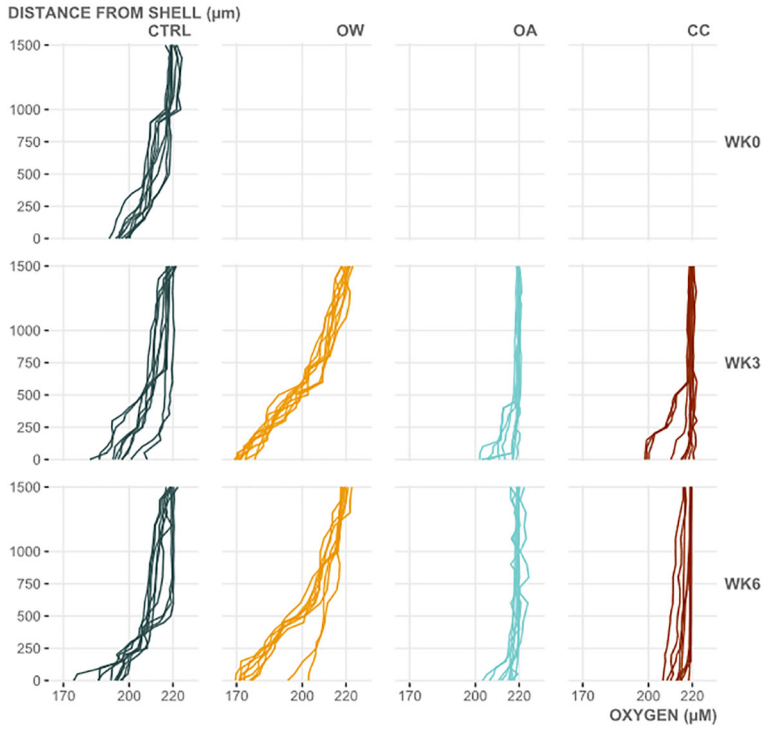

FIGURE 5
Vertical oxygen profiles of the microbial biofilm on *Mytilus edulis* shells, 1500µm above the shell surface, before seawater manipulations started (WK0) and after three and six weeks of manipulations (WK3 and WK6, respectively) in each experimental treatment [CTRL: control, OA: ocean acidification, OW: ocean warming and CC: climate change]. Profiles were measured on three random locations per replicate *M. edulis* shell (n=3) per timepoint and treatment.

shell. However, as the N_2O flux was several orders of magnitude lower than that of the other measured N species (NH_4^+, NO_2^- and NO_3^-), reduction of N_2O to N_2 must still have occurred to close the nitrogen budget in the experimental incubations. Research by Marzocchi et al. (2021) suggests that mussel-associated N_2 production, although currently often overlooked, might be substantial. The high CTRL nitrate consumption rates observed in this study comply with this assumption.

4.2 Climate change effects on N_2O production

By nature, adult blue mussels have a wide thermal tolerance window (e.g. Seuront et al., 2019; Kamermans and Saurel, 2022). Since this species has adapted to survive in such variable conditions, this study opted to push towards the boundaries of its natural tolerances in order to get the most realistic stress response to variable climate scenarios. In the North Sea, the highest mean temperatures occur over the summer period (when organisms were sampled) when the mean seawater pH is fairly stable (LifeWatch Belgium, 2015), meaning the adopted climate manipulations should elicit a relatively accurate physiological response outside *M. edulis*' natural tolerances. Results show that the effects of seawater temperature rise and ocean acidification were generally of an antagonistic nature. N_2O production rates of whole animals, as well as the production rate of dissected shells with an intact microbial biofilm, significantly increased with a higher temperature and significantly decreased in an acidified environment (whole animals) or a combined high temperature/low pH climate change environment (biofilm).

These experiments were set up to mimic North Sea summer conditions in CTRL, with additional manipulations in terms of temperature and/or pH levels according to the experimental treatments. Although this summer setting is the most relevant in terms of studying potential stress responses due to climate change, the temperature-dependent nature of physiological and microbial processes suggest that the absolute values of these responses would differ between the seasons (Lesser et al., 2010; Boulêtreau et al., 2012; Múgica et al., 2015). However, whether the observed patterns and nature of the interaction between ocean warming and acidification varies seasonally remains to be confirmed.

The increasing effect of elevated temperature on N_2O production rates by *M. edulis* and its associated shell biofilm are most likely linked to the mussel's concomitantly increasing filtration rates in combination with temperature-induced increased biofilm activity. As bivalve filter feeding increases with temperature (Kittner and Riisgård, 2005; Ong et al., 2017; Voet et al., 2021), more denitrifying microorganisms might be ingested and/or the concentration of available N precursors in the digestive system might increase. In addition, general microbial activity increases with warmer temperatures (Kroeze and Seitzinger, 1998; Boulêtreau et al., 2012). This study showed that even though the N_2O production by whole animals increased with temperature, the relative contribution of the microbial shell biofilm remained stable over time in the ocean warming [OW] scenario. Indeed, this would

suggest a similar positive effect of warmer environments on both the animal's and the shell biofilm's N_2O producing capacities. Moreover, increased feeding rates will result in higher biodeposition rates and in turn, a higher nutrient load, potentially further stimulating (de) nitrification activities in the microbial shell biofilm.

On the other hand, the relative contribution of the shell biofilm to N_2O production evidently decreased over time in both acidified scenarios, on top of the overall decrease in whole animal N_2O production rates. A negative effect of ocean acidification on the marine nitrogen cycle was previously observed by Beman et al. (2011), reporting reduced oceanic nitrification at even relatively small experimental pH reductions (0.05-0.14). Together with a profound effect of reduced pH on the community composition of marine biofilms (Espinel-Velasco et al., 2021), this could potentially explain the observed lower N_2O production rates under acidified conditions, as well as the decreasing relative contribution of the microbial biofilm. The latter is most likely also tied to a thinner, patchier or even disappearing shell biofilm, as is suggested by this study's significantly affected oxygen microprofiles in both acidified conditions. The microprofile analysis indeed confirmed an adverse effect of pH on the metabolic activity (respiration) and composition of the shell biofilm. In both acidified treatments, perceived biofilm thickness considerably decreased, as well as the net biofilm oxygen consumption. Furthermore, net oxygen consumption at the shell surface sometimes dropped to (near) zero under acidified conditions, indicating either an incomplete biofilm cover or a profound shift in functional metabolism and/or the biofilm's microbial makeup. A more in-depth functional analysis of *M. edulis'* shell biofilm under climate change conditions is described in more detail by Dairain et al. (manuscript in preparation)[2]. Nitrifier denitrification, shown to be the dominant N_2O producing pathway for *M. edulis* (e.g. this study and Heisterkamp et al., 2013), gained even more importance in the OA treatment. Affirmingly, this could (in part) be a result of the increasing prevalence of suboxic conditions provided within a thinning and/or receding shell biofilm.

4.3 Towards ecosystem-level effects

The blue mussel is by far the most abundant mollusc species colonising North Sea artificial hard substrates (Coolen et al., 2020) and these numbers will multiply even further by planned co-location strategies involving offshore wind farms and bivalve mariculture (Schupp et al., 2019; MSP, 2020; Steins et al., 2021). Considering the prevalence of these organisms and the potential biofilm-substrate they provide are on the rise, their role in the local emission of the potent GHG nitrous oxide could be noteworthy and a valuable research topic. On the other hand, this study also suggested that reduction of this GHG to inert N_2 could be prevalent in or around these mussels, as was the case in other recent mussel microbiome research (Marzocchi et al., 2021). This would suggest that colonising and aquaculture mussel communities could play a role in the removal of nitrogen from the water column, actively counteracting marine eutrophication. Contrary to climate change-induced changes in (i.a.) survival or ecophysiology of blue mussels (Voet et al., 2021), the antagonistic effects of temperature and pH on N_2O production described in this study would most likely not amount to large-scale enhancements of future mussel-associated N_2O emissions. With the expansion of the offshore renewable energy effort in a necessary attempt to abate GHG emissions causing global climate change, insights such as described in this study are paramount. Complementary, marine climate science would benefit greatly from further research into the link between impacts of future climate effects on current marine communities and the potential effects of adaptation and ecophysiological acclimatisation over longer time periods.

5 Conclusion

The blue mussel *Mytilus edulis* and its microbial shell biofilm produce N_2O through three potential pathways, i.e. nitrification, denitrification (CND) and nitrifier denitrification (using ammonium, nitrate and nitrite as a precursor, respectively), but nitrifier denitrification proved to be the main pathway. The relative importance of these pathways and the relative contribution of the shell biofilm to the blue mussel's total N_2O production, as well as the biofilm thickness, metabolic activity and coverage are all affected by warming, acidification, or the combination of both. The effects of temperature and pH were often of an antagonistic nature, predicting a relatively small net effect on local N_2O production in future climate environments. In a future setting with increasing blue mussel densities, such as proliferating offshore wind farms in possible multifunctional co-use with bivalve mariculture, animal-associated N_2O and N_2 production will play a major role in local nitrogen cycling and have potential knock-on effects on local greenhouse gas emissions, eutrophication levels and bioavailable nitrogen concentrations. An understanding of the underlying pathways and inner dynamics of the OWF- and aquaculture-bound N cycling will therefore be indispensable to face and mitigate the additional impact of a changing marine climate.

Data availability statement

The raw data supporting the conclusions of this article will be made available by the authors, without undue reservation.

Author contributions

HV: Conceptualization, Methodology, Validation, Formal analysis, Investigation, Resources, Data curation, Writing – original draft, Writing – review and editing, visualization. KS: Conceptualization, Methodology, Validation, Resources, Writing – review and editing, supervision, funding acquisition. TM:

2 Dairain, A., Voet, H. E. E., Vafeiadou, A.-M., de Meester, N., Rigaux, A., van Colen, C., et al. (manuscript in preparation). Structurally stable but functionally disrupted marine epi-microbial communities under a future climate change scenario: impact on the nitrogen cycle.

Methodology, Validation, Resources, Writing – review and editing, supervision, project administration. SB: Methodology, Formal analysis, Writing – review and editing. PB: Funding acquisition, Resources, Writing – review and editing. CC: Conceptualization, Methodology, Validation, Resources, Writing – review and editing, supervision, funding acquisition. JV: Conceptualization, Methodology, Validation, Resources, Writing – review and editing, supervision, project administration, funding acquisition. All authors contributed to the article and approved the submitted version.

Funding

The research leading to results presented in this publication was funded through BELSPO BRAIN-be project BR/175/A1/PERSUADE, additional funding obtained from Ghent University's Special Research Fund (BOF) through GOA project 01G02617 and carried out with infrastructure funded by EMBRC Belgium FWO project GOH3817N. This work was further supported by logistic support from the Research Vessel Simon Stevin, the vessel Stream (Brevisco), the scientific diving teams of VLIZ and RBINS and by access to the ILVO aquaculture pilot project Value@Sea (with partners Belwind, Brevisco, Sioen Industries, Colruyt Group, C-Power, DEME, RBINS – OD Nature, Lobster Fish and Ghent University). Practical and analytical support by the MarBiol Research Group (UGent), VLIZ, the Chemical Oceanography Unit (COU; University of Liège) and the Isotope Bioscience Laboratory (ISOFYS; UGent) was indispensable in the realisation of this study.

Conflict of interest

The authors declare that the research was conducted in the absence of any commercial or financial relationships that could be construed as a potential conflict of interest.

Publisher's note

Supplementary material

The Supplementary Material for this article can be found online at: https://www.frontiersin.org/articles/10.3389/fmars.2023.1101469/full#supplementary-material

References

Anderson, M. J., Gorley, R. N., and Clarke, K. R. (2008). PERMANOVA+ for PRIMER: guide to software and statistical methods. *Primer-E Plymouth*.

Avdelas, L., Avdic-Mravlje, E., Borges Marques, A. C., Cano, S., Capelle, J. J., Carvalho, N., et al. (2021). The decline of mussel aquaculture in the European union: causes, economic impacts and opportunities. *Rev. Aquacult.* 13, 91–118. doi: 10.1111/raq.12465

Bange, H. W., Freing, A., Kock, A., and Löscher, C. R. (2010). "Marine pathways to nitrous oxide," in *Nitrous oxide and climate change*. Ed. K. Smith (London: Earthscan), 36–62.

Bates, D., Maechler, M., Bolker, W., and Walker, S. (2015). Fitting linear mixed-effects models using lme4. *J. Stat. Softw.* 67 (1), 1–48. doi: 10.18637/jss.v067.i01

Belser, L. W., and Mays, E. L. (1980). Specific inhibition of nitrite oxidation by chlorate and its use in assessing nitrification in soils and sediments. *Appl. Environ. Microbiol.* 39, 505–510. doi: 10.1128/aem.39.3.505-510.1980

Beman, J. M., Chow, C.-E., King, A. L., Feng, Y., Fuhrman, J. A., Andersson, A., et al. (2011). Global declines in ocean nitrification rates as a consequence of ocean acidification. *Proc. Natl. Acad. Sci.* 108 (1), 208–213. doi: 10.1073/pnas.1011053108

Bindoff, N. L., Cheung, W. W. L., Kairo, J. G., Arístegui, J., Guinder, V. A., Hallberg, R., et al (2019) "Changing ocean, marine ecosystems, and dependent communities" in *IPCC special report on the ocean and cryosphere in a changing climate*. Eds. H. O. Pörtner, D. C. Roberts, V. Masson-Delmotte, P. Zhai, M. Tignor, E. Poloczanska, K. Mintenbeck, A. Alegría, M. Nicolai, A. Okem, J. Petzold, B. Rama and N. M. Weyer Cambridge University Press, Cambridge, UK and New York, NY, USA, 447–587. doi: 10.1017/9781009157964.007

Birkbeck, T. H., and McHenery, J. G. (1982). Degradation of bacteria by *Mytilus edulis*. *Mar. Biol.* 72, 7–15. doi: 10.1016/0305-0491(89)90174-0

Bonaglia, S., Brüchert, V., Callac, N., Vicenzi, A., Chi Fru, E., and Nascimento, F. J. A. (2017). Methane fluxes from coastal sediments are enhanced by macrofauna. *Nat. Sci. Rep.* 7 (1), 13145. doi: 10.1038/s41598-017-13263-w

Boulêtreau, S., Salvo, E., Lyautey, E., Mastrorillo, S., and Garabetian, F. (2012). Temperature dependence of denitrification in phototrophic river biofilms. *Sci. Total Environ.* 416, 323–328. doi: 10.1016/j.scitotenv.2011.11.066

Buck, B. H., and Langan, R. (2017). "Chapter 14: Epilogue–pathways towards sustainable ocean food production," in *Aquaculture perspective of multi-use sites in the open ocean*. Eds. B. H. Buck and R. Langan, Springer International Publishing, ISBN: 978-3-319-51159-7 395–404.doi: 10.1007/978-3-319-51159-7

Clarke, K. R., and Gorley, R. N. (2006). Primer v6: User Manual/Tutorial. *Primer-E Plymouth*.

Coolen, J. W. P., van der Weide, B., Cuperus, J., Blomberg, M., Van Moorsel, G. W. N. M., Faasse, M. A. A., et al. (2020). Benthic biodiversity on old platforms, young wind farms and rocky reefs. *ICES J. Mar. Sci.* 77 (3), 1250–1265. doi: 10.1093/icesjms/fsy092

Costello, C., Cao, L., Gelcich, S., Cisneros-Mata, M. A., Free, C. M., Froehlich, H. E., et al. (2020). The future of food from the sea. *Nature* 588, 95–100. doi: 10.1038/s41586-020-2616-y

Cranford, P. J. (2019). "Chapter 8: Magnitude and extent of water clarification services provided by bivalve suspension feeding," in *Goods and services of marine bivalves*. Eds. A. C. Smaal, J. G. Ferreira, J. Grant, J. K. Petersen and Ø Strand, Springer Cham 119–141. doi: 10.1007/978-3-319-96776-9

Degraer, S., Carey, D. A., Coolen, J. W. P., Hutchison, Z. L., Kerckhof, F., Rumes, B., et al. (2020). Offshore wind farm artificial reefs affect ecosystem structure and functioning: A synthesis. in special issue on understanding the effects of offshore wind energy development on fisheries. *Oceanography* 33 (4), 48–57. doi: 10.5670/oceanog.2020.405

De Mesel, I., Kerckhof, F., Norro, A., Rumes, B., and Degraer, S. (2015). Succession and seasonal dynamics of the epifauna community on offshore wind farm foundations and their role as stepping stones for non-indigenous species. *Hydrobiologia* 756, 37–50. doi: 10.1007/s10750-014-2157-1

Espinel-Velasco, N., Tobias-Hünefeldt, S. P., Karelitz, S., Hoffmann, L. J., Morales, S. E., and Lamare, M. D. (2021). Reduced seawater pH alters marine biofilms with impacts for marine polychaete larval settlement. *Mar. Env. Res.* 167, 105291. doi: 10.1016/j.marenvres.2021.105291

Foesel, B. U., Gieseke, A., Schwermer, C., Stief, P., Koch, L., Cytryn, E., et al. (2008). Nitrosomonas Nm143-like ammonia oxidizers and nitrospira marina-like nitrite oxidizers dominate the nitrifier community in a marine aquaculture biofilm. *FEMS Microbiol. Ecol.* 63 (2), 192–204. doi: 10.1111/j.1574-6941.2007.00418.x

Fox-Kemper, B., Hewitt, H. T., Xiao, C., GAðalgeirsdóttir, G., Drijfhout, S. S., Edwards, T. L., et al. (2021). "Ocean, cryosphere and Sea level change," in *Climate change 2021: The physical science basis. contribution of working group I to the sixth assessment report of the intergovernmental panel on climate change*. Eds. V. Masson-Delmotte, P. Zhai, A. Pirani, S. L. Connors, C. Péan, S. Berger, N. Caud, Y. Chen, L. Goldfarb, M. I. Gomis, M. Huang, K. Leitzell, E. Lonnoy, J. B. R. Matthews, T. K. Maycock, T. Waterfield, O. Yelekçi, R. Yu and B. Zhou (Cambridge University Press, Cambridge, United Kingdom and New York, NY, USA), 1211–1362. doi: 10.1017/9781009157896.011

Gárate, M., Moseman-Valtierra, S., and Moen, A. (2019). Potential nitrous oxide production by marine shellfish in response to warming and nutrient enrichment. *Mar. pollut. Bull.* 146, 236–246. doi: 10.1016/j.marpolbul.2019.06.025

GWEC (Global Wind Energy Council) (2021). *Global wind report 2021*. Eds. J. Lee, F. Zhao, A. Dutton, B. Backwell, R. Fiestas, L. Qiao, N. Balachandran, S. Lim, W. Liang, E. Clarke, A. Lathigara and D. R. Younger, 80.

Halekoh, U., and Højsgaard, S. (2014). A kenward-roger approximation and parametric bootstrap methods for tests in linear mixed models - the r package pbkrtest. *J. Stat. Softw.* 59 (9).

Heisterkamp, I. M., Schramm, A., de Beer, D., and Stief, P. (2010). Nitrous oxide production associated with coastal marine invertebrates. *Mar. Ecol. Prog. Ser.* 415, 1–9. doi: 10.3354/meps08727

Heisterkamp, I. M., Schramm, A., Larsen, L. H., Svenningsen, N. B., Lavik, G., de Beer, D., et al. (2013). Shell biofilm-associated nitrous oxide production in marine molluscs: processes, precursors and relative importance. *Environ. Microbiol.* 15 (7), 1943–1955. doi: 10.1111/j.1462-2920.2012.02823.x

Hoegh-Guldberg, O., Cai, R., Poloczanska, E. S., Brewer, P. G., Sundby, S., Hilmi, K., et al. (2014). "The ocean," in *Climate change 2014: Impacts, adaptation, and vulnerability. part b: Regional aspects. contribution of working group II to the fifth assessment report of the intergovernmental panel on climate change*. Eds. V. R. Barros, C. B. Field, D. J. Dokken, M. D. Mastrandrea, K. J. Mach, T. E. Bilir, M. Chatterjee, K. L. Ebi, Y. O. Estrada, R. C. Genova, B. Girma, E. S. Kissel, A. N. Levy, S. MacCracken, P. R. Mastrandrea and L. L. White (Cambridge, United Kingdom and New York, NY, USA: Cambridge University Press), 1655–1731.

IEA (International Energy Agency) (2019). *Offshore wind outlook* (Copenhagen, Denmark).

IPCC (2021). "Summary for policymakers," in *Climate change 2021: The physical science basis. contribution of working group I to the sixth assessment report of the intergovernmental panel on climate change*. Eds. V. Masson-Delmotte, P. Zhai, A. Pirani, S. L. Connors, C. Péan, S. Berger, N. Caud, Y. Chen, L. Goldfarb, M. I. Gomis, M. Huang, K. Leitzell, E. Lonnoy, J. B. R. Matthews, T. K. Maycock, T. Waterfield, O. Yelekçi, R. Yu and B. Zhou (Cambridge University Press, United Kingdom and New York, NY, USA, In press). doi: 10.1017/9781009157896

Ivanov, E., Capet, A., De Borger, E., Degraer, S., Delhez, E. J. M., Soetaert, K., et al. (2021). Offshore wind farm footprint on organic and mineral particle flux to the bottom. *Front. Mar. Sci.* 8, 631799. doi: 10.3389/fmars.2021.631799

Kamermans, P., and Saurel, C. (2022). Interacting climate change effects on mussels (Mytilus edulis and m. galloprovincialis) and oysters (Crassostrea gigas and ostrea edulis): experiments for bivalve individual growth models. *Aquat. Living Resour.* 35 (1). doi: 10.1051/alr/2022001

Kittner, C., and Riisgård, H. U. (2005). Effect of temperature on filtration rate in the mussel *Mytilus edulis*: no evidence for temperature compensation. *Mar. Ecol. Prog. Ser.* 305, 147–152. doi: 10.3354/meps305147

Kroeze, C., and Seitzinger, S. P. (1998). Nitrogen inputs to rivers, estuaries and continental shelves and related nitrous oxide emissions in 1990 and 2050: a global model. *Nutr. Cycl. Agroecosyst.* 52, 195–212. doi: 10.1023/A:1009780608708

Lesser, M., Bailey, M., Merselis, D., and Morrison, J. (2010). Physiological response of the blue mussel mytilus edulis to differences in food and temperature in the gulf of Maine. *Comp. Biochem. Physiol. Part A Mol. Integr. Physiol.* 156, 541–551. doi: 10.1016/j.cbpa.2010.04.012

LifeWatch Belgium (2015) *Flanders Marine institute. Thornton measuring buoy (C-power)*. Available at: https://rshiny.lifewatch.be/buoy-data/ (Accessed 30 June 2018).

Marzocchi, U., Bonaglia, S., Zaiko, A., Quero, G. M., Vybernaite-Lubiene, I., Politi, T., et al. (2021). Zebra mussel holobionts fix and recycle nitrogen in lagoon sediments. *Front. Microbiol.* 11. doi: 10.3389/fmicb.2020.610269

Mehrbach, C., Culberson, C. H., Hawley, J. E., and Pytkowicz, R. M. (1973). Measurement of the apparent dissociation constants of carbonic acid in seawater at atmospheric pressure. *Limnol. Ocean* 18, 897–907. doi: 10.4319/lo.1973.18.6.0897

Mosier, A., Kroeze, C., Nevison, C., Oenema, O., Seitzinger, S., and Van Cleemput, O. (1998). Closing the global N2O budget: nitrous oxide emissions through the agricultural nitrogen cycle — OECD/IPCC/IEA phase II development of IPCC guidelines for national greenhouse gas inventory methodology. *Nutr. Cycl. Agroecosyst.* 52, 225–248. doi: 10.1023/A:1009740530221

MSP – Marine Spatial Plan 2020-2026 (2020) *Marine environment service, federal public service – health, food chain safety and environment*. Available at: https://www.health.belgium.be/en/environment/seas-oceans-and-antarctica/north-sea-and-oceans/marine-spatial-plan (Accessed 1 June 2021).

Múgica, M., Sokolova, I. M., Izagirre, U., and Marigómez, I. (2015). Season-dependent effects of elevated temperature on stress biomarkers, energy metabolism and gamete development in mussels. *Mar. Environ. Res.* 103, 1–10. doi: 10.1016/j.marenvres.2014.10.005

Myhre, G., Shindell, D., Bréon, F.-M., Collins, W., Fuglestvedt, J., Huang, J., et al. (2013). "Anthropogenic and natural radiative forcing," in *Climate change 2013: The physical science basis. contribution of working group I to the fifth assessment report of the intergovernmental panel on climate change*. Eds. T. F. Stocker, D. Qin, G.-K. Plattner, M. Tignor, S. K. Allen, J. Boschung, A. Nauels, Y. Xia, V. Bex and P. M. Midgley (Cambridge, United Kingdom and New York, NY, USA: Cambridge University Press), 659–740.

Ong, E. Z., Briffa, M., Moens, T., and Van Colen, C. (2017). Physiological responses to ocean acidification andwarming synergistically reduce condition of the common cockle Cerastoderma edule . *Marine Environmental Research* . doi: 10.1016/j.marenvres.2017.07.001

Pierrot, D., Lewis, E., and Wallace, D. W. R. (2006). MS Excel Program Developed for CO2System Calculations. ORNL/CDIAC-105a. Carbon Dioxide Inf. Anal. Center, Oak Ridge Natl. Lab. US Dep. Energy, Oak Ridge, Tennessee.

R Core Team (2019). *R: A language and environment for statistical computing. r foundation for statistical computing* (Vienna, Austria).

Schramm, A., De Beer, D., Gieseke, A., and Amann, R. (2000). Microenvironments and distribution of nitrifying bacteria in a membrane-bound biofilm. *Environ. Microbiol.* 6), 680–686. doi: 10.1046/j.1462-2920.2000.00150.x

Schupp, M. F., Bocci, M., Depellegrin, D., Kafas, A., Kyriazi, Z., Lukic, I., et al. (2019). Towards a common understanding of ocean multi-use. *Front. Mar. Sci.* 6, 165. doi: 10.3389/fmars.2019.00165

Seuront, L., Nicastro, K. R., Zardi, G. I., and Goberville, E. (2019). Decreased thermal tolerance under recurrent heat stress conditions explains summer mass mortality of the blue mussel *Mytilus edulis*. *Sci. Rep.* 9, 17498. doi: 10.1038/s41598-019-53580-w

Shrestha, N. K., Hadano, S., Kamachi, T., and Okura, I. (2002). Dinitrogen production from ammonia by nitrosomonas europaea. *Appl. Catal. A: Gen.* 237 (1-2), 33–39. doi: 10.1016/S0926-860X(02)00279-X

Slavik, K., Lemmen, C., Zhang, W., Kerimoglu, O., Klingbeil, K., and Wirt, K. W. (2019). The large-scale impact of offshore wind farm structures on pelagic primary productivity in the southern north Sea. *Hydrobiologia* 845, 35–53. doi: 10.1007/s10750-018-3653-5

Smith, H. A., and Sharp, K. (2012). Indigenous climate knowledges. *Wiley Interdiscip. Rev.: Climate Change* 3 (5), 467–476. doi: 10.1002/wcc.185

Stein, L. Y., and Yung, Y. L. (2003). Production, isotopic composition, and atmospheric fate of biologically produced nitrous oxide. *Annu. Rev. Earth Planet Sci.* 31, 329–356. doi: 10.1146/annurev.earth.31.110502.080901

Steins, N. A., Veraart, J. A., Klostermann, J. E. M., and Poelman, M. (2021). Combining offshore wind farms, nature conservation and seafood: Lessons from a Dutch community of practice. *Mar. Policy* 126, 104371. doi: 10.1016/j.marpol.2020.104371

Stief, P., Poulsen, M., Nielsen, L. P., Brix, H., and Schramm, A. (2009). Nitrous oxide emission by aquatic macrofauna. *Proc. Natl. Acad. Sci. U.S.A.* 106, 4296–4300. doi: 10.1073/pnas.0808228106

Tallec, G., Garnier, J., Billen, G., and Gousailles, M. (2008). Nitrous oxide emissions from denitrifying activated sludge of urban wastewater treatment plants, under anoxia and low oxygenation. *Bioresour. Technol.* 99 (7), 2200–2209. doi: 10.1016/j.biortech.2007.05.025

Voet, H. E. E., Van Colen, C., and Vanaverbeke, J. (2021). Climate change effects on the ecophysiology and ecological functioning of an offshore wind farm artificial hard substrate community. *Sci. Total Environ.* 810, 152194. doi: 10.1016/j.scitotenv.2021.152194

Widdicombe, S., Beesley, A., Berge, J. A., Dashfield, S. L., McNeill, C. L., Needham, H. R., et al. (2013). Impact of elevated levels of CO2 on animal mediated ecosystem function: The modification of sediment nutrient fluxes by burrowing urchins. *Mar. pollut. Bull.* 73 (2), 416–427. doi: 10.1016/j.marpolbul.2012.11.008

Zhu, X., Burger, M., Doane, T. A., and Horwath, W. (2013). Ammonia oxidation pathways and nitrifier denitrification are significant sources of N2O and NO under low oxygen availability. *Proc. Natl. Acad. Sci.* 110 (16), 6328–6333. doi: 10.1073/pnas.1219993110